Phenylalanyl and Tyrosyl Side-Chain Mobility in the M13 Coat Protein Reconstituted in Phospholipid Vesicles†

Heather D. Dettman, Joel H. Weiner, and Brian D. Sykes*

ABSTRACT: Analyses of the internal motions of proteins have increased our knowledge of protein structure in relation to function. These analyses have been done, primarily, for water-soluble proteins, whose amino acid residues may experience two types of environments: the aqueous solvent outside or the hydrophobic core inside the protein. Residues on membrane proteins may be influenced by yet a third type of environment, that provided by the surrounding lipids. Quantitation of the motions within membrane proteins is required to determine the extent to which this third environment contributes to membrane protein structure/activity. We have studied the behavior of the major coat protein of the filamentous coliphage, M13, when reconstituted into vesicles consisting of 80% dimyristoylphosphatidylcholine, 10% cardiolipin, and 10% dipalmitoylphosphatidic acid, by weight. The protein had been labeled, in vivo, with 3-fluoro analogues of phenylalanine and tyrosine, thus providing specific labels of the hydrophilic and hydrophobic regions of the protein, respectively, for study using ^{19}F NMR (nuclear magnetic resonance). To determine the exposure and orientation of the vesicle-bound coat protein, chymotryptic digestion and temperature experiments were done. Chymotryptic digestion, monitored by ^{19}F NMR and paper electrophoresis, showed that the protein was incorporated symmetrically, as both the N- and C-terminal F-Phe residues were susceptible to the protease. The F-Tyr residues though were protected by the lipid bilayer. Temperature studies, where an 8-fluoro analogue of dipalmitoylphosphatidylcholine was included as a lipid probe, demonstrated that the motions of both the F-Tyr and 8-FDPPC were affected by the fluidity state of the lipid, while the F-Phe mobility was not. These experiments confirm that the F-Phe and F-Tyr labels are reporting from the aqueous and bilayer environments, respectively. Quantitation of the ring motions of the F-Phe and F-Tyr residues was done through computer simulation of the ^{19}F NMR resonance line width, NOE (nuclear Overhauser effect), and T_1 data, measured at 303 K. The computer algorithm was based upon a model allowing the residue rings to wobble about the $\alpha\beta$-bond and rotate about the $\beta\gamma$-bond; the overall vesicle tumbling was assumed to have spherical symmetry. It was found that both the F-Phe and F-Tyr data were most closely simulated when the wobble frequency about the $\alpha\beta$-bond was 2×10^8 s^{-1} and the rotation frequency about the $\beta\gamma$-bond was 4×10^8 s^{-1}. Both residues also seem to interact with neighboring molecules: the F-Tyr with passing lipids while the F-Phe with either phospholipid head groups or other amino acids. The difference between the two residues was in the angle through which the rings wobbled: the F-Tyr ring wobble angle was ±75° while the F-Phe angle was ±90°. As well, there is greater backbone motion for the hydrophilic ends containing the F-Phe residues relative to the transmembranal region, where the F-Tyr residues are found. Although the hydrophilic termini are allowed larger amplitudes of motion compared to the region of the protein surrounded with lipids, they are not freely moving about in solution but are either themselves structured or otherwise being restricted at the membrane surface. In turn, the motions found for the F-Tyr residues are comparable to those of a tyrosine buried in a hydrophobic pocket of a water-soluble protein. This indicates that surrounding a residue with lipids in the liquid-crystalline state is not more restrictive than surrounding a residue with other amino acid side chains.

In recent years, there has been considerable interest in the internal motions of the amino acid residues of proteins. Most work has been done on water-soluble proteins, which tend to be the best characterized, the most available, and the easiest to study [for a recent review, see Jardetzky & Roberts (1981)]. Membrane-bound proteins have been much less studied (Kinsey et al., 1981). For these proteins, the mobility of individual residues is influenced by both the secondary and tertiary structure of the protein and the structure of and interaction with the surrounding lipids.

Nuclear magnetic resonance (NMR)[1] spectroscopy is a technique by which motions within the protein may be studied. Analyses of ^1H, ^{13}C, and ^{31}P NMR spectra obtained from biological molecules have provided useful information about the internal motions of macromolecules. For membrane-bound proteins, however, these particular nuclei have limited use for two reasons. First, the membranes containing the proteins are large, and consequently, broad NMR resonances are obtained. Second, there are many proton, carbon, and phosphorus nuclei present, so that it is difficult to resolve the resonance from a particular nucleus within the system. A nucleus that we have found particularly valuable in circumventing these problems is fluorine-19 (Weiner & Sykes, 1980). The ^{19}F nucleus, as well as being highly abundant (100%), is highly sensitive; its gyromagnetic ratio is 0.94 times that of ^1H. Fluorine is not commonly found in biological systems so that no background resonances are present. The use of fluoro amino acid analogues provides specific labels within the macromolecule of interest. This, combined with the large chemical shift range of ^{19}F NMR, means that detailed analyses of specific regions of the biological molecule are possible.

As a model system for the study of the internal side-chain motions of residues in membrane-bound proteins, we have been

† From the Medical Research Council Group on Protein Structure and Function, Department of Biochemistry, University of Alberta, Edmonton, Alberta T6G 2H7, Canada. *Received June 16, 1983.* Supported by the MRC Group in Protein Structure and Function and MRC Grant MT5838.

[1] Abbreviations: NMR, nuclear magnetic resonance; DOC, sodium deoxycholate; F-Phe, 3-fluorophenylalanine; F-Tyr, 3-fluorotyrosine; 8-FDPPC, 8-fluorodipalmitoylphosphatidylcholine; DMPC, dimyristoylphosphatidylcholine; DPPA, dipalmitoylphosphatidic acid; CL, cardiolipin; SUV, small unilamellar vesicle; T_1, spin–lattice relaxation time; $\Delta\nu$, Lorentzian line width at half the peak height; NOE, nuclear Overhauser effect.

0006-2960/84/0423-0705$01.50/0

studying the coat (gene 8) protein of the filamentous coliphage M13 [see Hagen et al. (1978, 1979a,b) and Dettman et al. (1982)]. Opella and co-workers have done a considerable amount of work on the coat protein of the very similar phage, fd, using ^{1}H, ^{2}H, ^{13}C, ^{15}N and ^{31}P NMR (Cross & Opella, 1979, 1980, 1981; Gall et al., 1981, 1982). During infection, the coat protein accumulates as a transmembranal protein in the inner membrane of *Escherichia coli*. The 50 amino acids of the coat protein (Dettman et al., 1982) can be divided into three domains: an acidic N-terminus, a basic C-terminus, and a hydrophobic core. We have used *E. coli* auxotrophs for in vivo replacement of the phenylalanines in the hydrophilic regions of the protein with 3-fluorophenylalanine and of the tyrosines in the hydrophobic domain with 3-fluorotyrosine. These labeled proteins have subsequently been incorporated into synthetic phospholipid vesicles. This paper presents the measurement and analysis of the ^{19}F NMR relaxation parameters (T_1, $\Delta\nu$, and NOE) for the F-Phe and F-Tyr residues of the coat protein of M13 in reconstituted vesicles. In addition ^{19}F NMR measurements are reported for fluorine-labeled lipid probes in these samples. This allows the simultaneous observation of the motional properties of the hydrophobic and hydrophilic portions of the protein and of the lipids in which the protein is embedded.

Theory

The overall goal of this paper is to quantitate the internal mobility of the side-chain residues of a membrane-bound protein from an analysis of NMR relaxation parameters ($\Delta\nu$, T_1, and NOE) measured as a function of resonance frequency. In the derivation of the equations that relate the experimentally measured variables to the parameters that characterize the motions within the system, two approaches are possible [for recent reviews, see London (1980) and Jardetzky & Roberts (1981)]. The first approach is to make no assumptions about what kinds of motion are present; the second is to assume a particular physical model for the motions. We have chosen the second approach for two reasons. First, it limits the number of variable parameters by fixing the bond angles around which motions are allowed and only letting the time scales of the motions be unknowns. This is necessary in our case given that only a limited number of measurements are possible and two relaxation mechanisms are present. The second reason for choosing the model-dependent approach is that the contributions of the various time scales determined with the model-independent approach are invariably rationalized in retrospect in terms of the physically most meaningful model for the motions. Time scales of the same orders of magnitude are extracted from the data in either case.

The model we have used for the possible motions is shown in Figure 1. This model allows restricted rotation (or wobble) about the $\alpha\beta$-bond of the aromatic ring of the amino acid side chain, free rotation about the $\beta\gamma$-bond, and overall spherical symmetry for vesicle rotation. Other motions of the α-carbon backbone of the protein with the vesicle such as lateral diffusion are, of course, possible and can be incorporated into this model by reducing the effective overall rotational correlation time for the protein. Further, experimental evidence from solid-state NMR (Gall et al., 1982) indicates that rapid vibration of the aromatic ring coupled with rarer 180° flips may be a better model than free diffusion for rotation about the $\beta\gamma$-bond.

The derivations of the equations of motion are outlined by Wittebort & Szabo (1978). We have extended their equations to include chemical shift anisotropy as a relaxation mechanism. Dipolar interactions are calculated between the fluorine nuclei

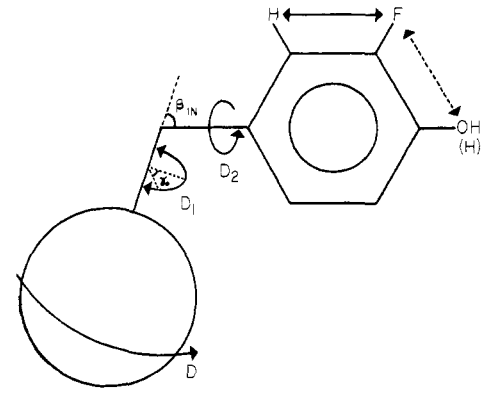

FIGURE 1: Diagram of rotations, angles, and possible dipolar interactions of the model assumed for the analysis of the F-Phe and F-Tyr relaxation data.

and the adjacent ring protons only. The dipole–dipole contribution to the spin–lattice and spin–spin relaxation rates is given by

$$1/T_1^{DD} = KF_1 \qquad 1/T_2^{DD} = (K/2)F_2$$

where

$$K = (1/10)\gamma_F^2\gamma_H^2\hbar^2/r_{F\text{-}H}^6$$

$$F_1 = J(\omega_F - \omega_H) + 3J(\omega_F) + 6J(\omega_F + \omega_H)$$

$$F_2 = F_1 + 4J(0) + 6J(\omega_H)$$

$$J(\omega) = \sum_{n=0}^{9}\sum_{b_1b_2=-2}^{2}[f_{nb_2}/(f_{nb_2}^2 + \omega^2)]\tilde{\Gamma}_{b_1b_1n}(\gamma_0) \times [d_{b_1b_2}(\beta_{1N})]^2[d_{b_20}(\beta_{NF})]^2$$

$$f_{nb_2} = 6D + D_1n^2\pi^2/(4\gamma_0^2) + b_2^2D_2$$

For $n = 0$

$$\tilde{\Gamma}_{b_1b_1n}(\gamma_0) = \sin^2(b_1\gamma_0)/(b_1\gamma_0)^2$$

For $n \geq 1$

$$\tilde{\Gamma}_{b_1b_1n}(\gamma_0) = \frac{b_1^2\gamma_0^2[\cos^2(b_1\gamma_0)[1 - (-1)^n] + \sin^2(b_1\gamma_0)[1 + (-1)^n]]}{[b_1^2\gamma_0^2 - (n\pi/2)^2]^2}$$

The chemical shift anisotropy contributions to the relaxation rate are given by

$$1/T_1^{CSA} = (6/40)\gamma_F^2H_0^2\delta_Z^2\sum_{b_2=0}^{2}\sum_{n=0}^{9}C_{b_2n}J_{b_2n}(\omega_F)$$

$$1/T_2^{CSA} = (1/40)\gamma_F^2H_0^2\delta_Z^2\sum_{b_2=0}^{2}\sum_{n=0}^{9}C_{b_2n}[3J_{b_2n}(\omega_F) + 4J_{b_2n}(0)]$$

where

$$J_{b_2n}(\omega) = 2f_{b_2n}/(f_{b_2n}^2 + \omega^2)$$

$$f_{b_2n} = 6D + n^2\pi^2D_1/(4\gamma_0^2) + b_2^2D_2$$

$$C_{b_2n} = \sum_{b_1=-2}^{2}\tilde{\Gamma}_{b_1b_1n}(\gamma_0)[d_{b_1b_2}(\beta_{1N})]^2C_{b_2}$$

For C_{b_2}:

$$C_0 = (1/4)[(3\cos^2\beta - 1) + \eta\sin^2\beta\cos(2\gamma)]^2$$

$$C_1 = (1/3)\sin^2\beta[\cos^2\beta[3 - \eta\cos(2\gamma)]^2 + \eta^2\sin^2(2\gamma)]$$

$$C_2 = [(3/4)^{1/2}\sin^2\beta + (\eta/[2(3)^{1/2}]) \times (1 + \cos^2\beta)\cos(2\gamma)]^2 + (\eta^2/3)\sin^2(2\gamma)\cos^2\beta$$

If one neglects cross-correlation between the two relaxation mechanisms, the total relaxation rates are given by

$$1/T_1 = 1/T_1^{DD} + 1/T_1^{CSA}$$

$$\Delta\nu = 1/(\pi T_2) = (1/\pi)(1/T_2^{DD} + 1/T_2^{CSA})$$

The NOE for F-Phe is given by

$$\frac{\gamma_H}{\gamma_F}\frac{\sigma_{H_2F} + \sigma_{H_4F}}{\rho_{H_2F}^{DD} + \rho_{H_4F}^{DD} + \rho^{CSA}} = \frac{\gamma_H}{\gamma_F}\frac{\sigma_{H_2F} + \sigma_{H_4F}}{1/T_1^{F\text{-}Phe}}$$

and for F-Tyr is given by

$$\frac{\gamma_H}{\gamma_F}\frac{\sigma_{HF}}{\rho^{DD} + \rho^{CSA}} = \frac{\gamma_H}{\gamma_F}\frac{\sigma_{HF}}{1/T_1^{F\text{-}Tyr}}$$

The nomenclature is that of Hull & Sykes (1974, 1975a,b) and Wittebort & Szabo (1978), where γ_F and γ_H are the fluorine and proton gyromagnetic ratios, respectively, ω_F and ω_H are the fluorine and proton resonance frequencies, respectively, $D = 1/(6\tau_c)$ where τ_c is the overall rotational correlation time for the protein, D_1 is the wobble frequency about the $\alpha\beta$-bond, D_2 is the ring rotation frequency about the $\beta\gamma$-bond, and γ_0 is the angle through which the ring "wobbles" (see Figure 1).

Materials and Methods

The F-Phe- and F-Tyr-labeled coat proteins were synthesized in vivo as outlined previously (Dettman et al., 1982). Protein was incorporated into phospholipid vesicles composed of 80% DMPC, 10% CL, and 10% DPPA by the cholate dialysis procedure described in the same paper except that the vesicle dialysis time was extended from 24 to 71 h to obtain a protein to cholate ratio of 10:1 in the final NMR sample. This ratio was determined by measuring the protein content with the Hartree protein assay (Hartree, 1972) and by monitoring the cholate concentration with [2,4-^{3}H]cholic acid obtained from New England Nuclear (Lachine, Quebec). The lipid content was measured by the procedure given by Raheja et al. (1973). The lipid to protein ratio determined for these vesicles was 54 ± 8.

Chymotryptic cleavage of the membrane-bound protein was performed with bovine pancreatic α-chymotrypsin from Sigma Chemical Co. (St. Louis, MO). The digestion procedure is outlined in the legend to Figure 3. The hydrophilic fragments were isolated as follows: the digested vesicles were separated from the fragments on an S-200 column (24 × 1.7 cm). The tubes containing the cleaved fragments were pooled and lyophilized. This fraction was then taken up in H_2O and lyophilized twice. A 0.5-mL aliquot of 0.1 M NH_4HCO_3–8 mM sodium deoxycholate was added to solubilize any lipid present. The DOC was then precipitated with the addition of 0.5 mL of 0.5 M formic acid and was pelleted by centrifugation in a Fisher Model 59 (benchtop) centrifuge for 5 min at 5000*g*. (This precipitation step removes lipid contamination and therefore prevents streaking of the subsequent electrophoresis.) The pellet was resuspended once in 1 mL of 0.5 M formic acid and recentrifuged. The supernatants were pooled and dried. They were then taken up in 0.5 mL of H_2O and redried 3 times. The paper electrophoresis procedure used was outlined previously (Dettman et al., 1982).

The vesicles used in the temperature studies were prepared as above except that 395 mg of DMPC was used rather than 400 mg. In the first experiments shown, 4 mg of 8-fluorodipalmitoylphosphatidylcholine was included to make the fluoro-lipid concentration 0.8% of the total lipid by weight. In the second set, the vesicles were made with the 8-FDPPC concentration increased to 2.4%. Temperatures were varied pseudorandomly to confirm the reversibility of the effects seen. The 8-FDPPC was obtained as a gift from Dr. R. McElhaney, University of Alberta, Edmonton, Alberta, Canada.

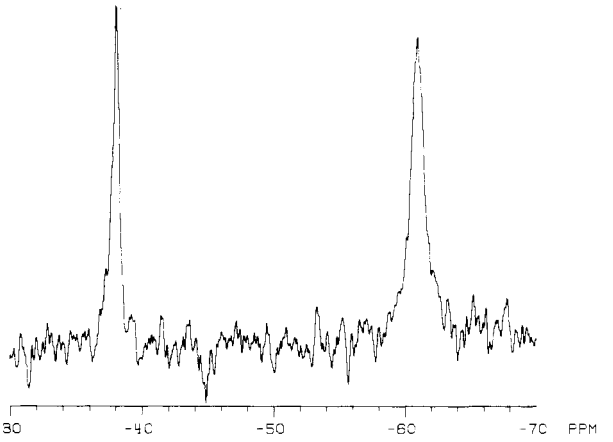

FIGURE 2: 254-MHz ^{19}F NMR spectrum of phospholipid vesicles containing equimolar quantities of F-Phe- and F-Tyr-labeled M13 coat protein. The spectrum was collected with a pulse width of 13 μs (69°), a sweep width of ±6300 Hz, and 4K data points, with a delay of 200 ms between transients. It is the result of 30 000 scans at 25-Hz line broadening.

^{19}F NMR experiments at 254 MHz were run on a Bruker HXS-270 NMR spectrometer operating in the Fourier-transform mode. Temperature regulation was maintained with the Bruker variable-temperature controller. The acquisition parameters are given in the figure legends. All line widths reported are the observed line widths minus the line broadening used by the computer as an exponential weighting function to improve the signal to noise of the spectrum. The other spectrometers used to determine the frequency dependence of the relaxation parameters are as follows: The 141-MHz spectra were taken on a Nicolet NT150 NMR spectrometer. The 376-MHz spectrum was run on a Bruker WH400 spectrometer. All chemical shifts reported are relative to sodium trifluoroacetate in D_2O, pH 7.0. The T_1's were measured by progressive saturation. The NOE data were obtained through broad-band irradiation of the entire proton spectrum and by observing the effect on the fluorine resonances. The decoupler was on prior to data acquisition so the spectra were not proton decoupled. A negative NOE indicates a decrease in signal intensity of the irradiated spectrum compared to that of the normal spectrum.

Results

Figure 2 shows the ^{19}F NMR spectrum of vesicles containing both F-Phe- and F-Tyr-labeled coat protein at 303 K. The assignments are based upon the shifts obtained for the free amino acids. The protein F-Phe and F-Tyr resonances are at −38.03 and −60.96 ppm while free F-Phe and F-Tyr peaks are found at −38.43 and −61.45 ppm. *J* coupling to protons is not resolved due to the broadness of the peaks.

The coat protein contains three phenylalanine and two tyrosine residues. As with all nuclei studied by NMR, the chemical shifts of the ^{19}F resonances reflect the local magnetic environments of the nuclei. If the three F-Phe's were in different environments, one would expect to resolve three peaks in the F-Phe region; similarly, one would expect to see two peaks in the F-Tyr region of the spectrum. Three F-Phe and two F-Tyr resonances have been resolved for the coat protein when it is dissolved in DOC micelles through the use of chymotryptic cleavage and temperature studies (Dettman et al., 1982). Vesicle-bound protein, however, does not appear

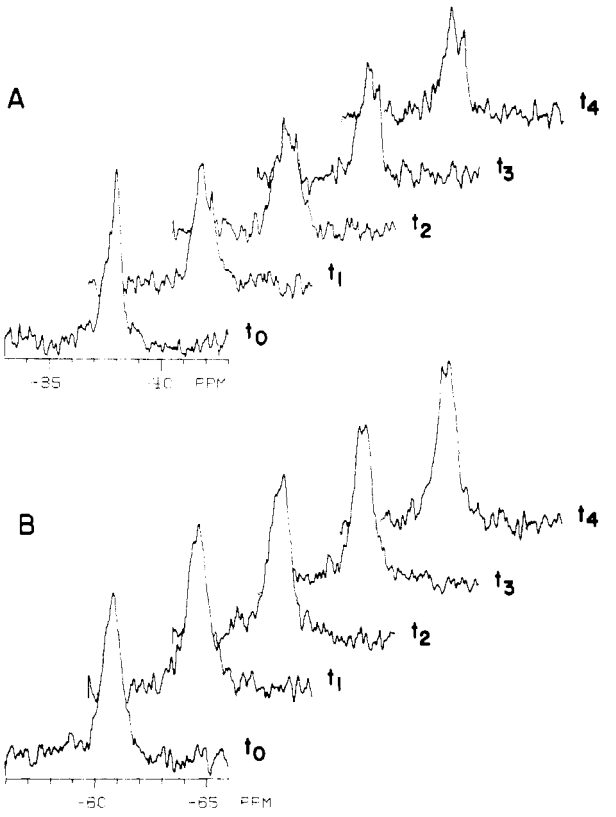

FIGURE 3: 254-MHz ^{19}F NMR spectra of the chymotryptic digestion of the F-Phe- and F-Tyr-labeled M13 coat protein reconstituted into vesicles. (A) Release of F-Phe fragments; (B) F-Tyr spectra during digestion. The digestion was done at 309 K with a chymotrypsin concentration of 67 μg/mL. The spectra were collected with a pulse width of 14 μs (74°), a sweep width of ±6300 Hz, and 4K data. The delay between transients was 200 ms, the line broadening was 20 Hz, and 10000 scans were taken per spectrum. Spectrum t_0 was collected before chymotrypsin was added. Spectra t_1–t_4 were collected at the following times after enzyme addition: (t_1) 0.5 h, (t_2) 1.5 h, (t_3) 2.5 h, and (t_4) 3.5 h.

to have this heterogeneity in chemical shift, even in the chymotryptic digestion and temperature experiments (see below). On this basis, the vesicle-bound protein F-Phe and F-Tyr resonances have been analyzed as single resonances with respect to chemical shift.

Experiments involving chymotryptic digestion of vesicles containing F-Phe- and F-Tyr-labeled coat proteins were performed to determine the exposure of the F-Phe and F-Tyr residues to the aqueous medium outside the vesicles and to obtain information about the orientation of the protein in the lipid bilayer. The results of this digestion are shown in Figure 3. Figure 3A shows the decrease of the area of the F-Phe protein resonance at −38.0 ppm with the concomitant appearance of a free F-Phe peptide resonance at −38.5 ppm. The relative areas of the protein and peptide resonances cannot be compared as care was not taken to prevent saturation of the peptide resonance; spectral parameters were optimized for collection of the protein resonance, which has a shorter T_1 than the peptide resonance. Comparison of either resonance as a function of time is however valid. Comparison of the area under the F-Phe protein resonance before the addition of chymotrypsin to that of the protein resonance after 3.5 h of digestion indicates that one-third of the F-Phe's have been cleaved. Chymotrypsin predominantly cleaves at the C-terminal side of exposed phenylalanine and tyrosine residues. The Phe cleavage sites of the coat protein are available when it is in DOC micelles; the Tyr sites are not exposed (Dettman et al., 1982). When the protein is in membrane vesicles, only

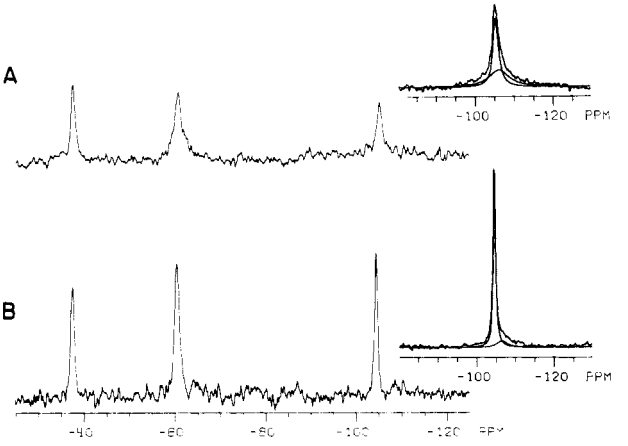

FIGURE 4: ^{19}F NMR spectra of F-Phe- and F-Tyr-labeled M13 coat protein reconstituted into 8-FDPPC-labeled phospholipid vesicles (see Materials and Methods). The spectra were collected with a pulse width of 12 μs (64°), a sweep width of ±50000 Hz, 8K data points, and delay of 300 ms between transients. (A) Result of 40000 scans at 292 K; (B) 20000 scans at 317 K. The inset resonances are those of 8-FDPPC from vesicles prepared with the 8-FDPPC concentration increased to 2.4% by weight. The upper inset was the result of 30000 scans at 292 K while the lower was of 15000 transients at 317 K. The broad and narrow spectral components of these resonances, as obtained from computer simulations, are shown by smooth curves.

half of the protein termini are exposed; the other half are protected inside the vesicle. Thus, one-third of the F-Phe residues would be released, regardless of the orientation of the protein in the membrane: exposed N-termini would be cleaved at F-Phe-11, releasing F-Phe-11, while exposed C-termini would be cleaved at F-Phe-42 and F-Phe-45, releasing F-Phe-45. In both orientations, two phenylalanines would be left with the vesicle-bound protein. Paper electrophoresis of the peptide fragments released showed that fragments were obtained from both the N- and C-termini (data not shown). These results have been referred to previously (Dettman et al., 1982). At that time, digestion of vesicle-bound protein could not be seen for vesicles that had been prepared with 8 M urea in the cholate buffer [the procedure that had been used by Hagen et al. (1978)]. It was suggested that the urea was altering the protein structure, perhaps through carbamylation of lysine side chains, and was rendering the protein indigestible to both chymotrypsin and Pronase (Dettman et al., 1982). Since that time, the preparation technique has improved and, hence, the signal to noise in the ^{19}F NMR spectra. We have found that samples prepared with 8 M urea in the cholate buffer are digestible by chymotrypsin with the same results as described above.

Figure 3B shows the F-Tyr region of the spectra during digestion. There is no release of F-Tyr-containing peptides seen in these spectra (these would have been seen at −61.8 ppm); nor is tyrosine found in the amino acid analysis of the fragments. It is apparent, however, that the release of the F-Phe peptides causes a change in the environment of the F-Tyr residues as indicated by the change in line shape with digestion.

Temperature studies were done with vesicles containing F-Phe- and F-Tyr-labeled protein and the monofluorinated lipid 8-FDPPC. Examples of two of the spectra collected are shown in Figure 4, the 8-FDPPC resonance appearing at −104.7 ppm. Comparison of the spectrum obtained at 317 K with that obtained at 292 K indicates that all three resonances, but particularly the F-Tyr and the 8-FDPPC resonances, are broader at the lower temperature. In addition to the line broadening at the lower temperatures, a change in line shape was observed. With the signal to noise of the spectra shown,

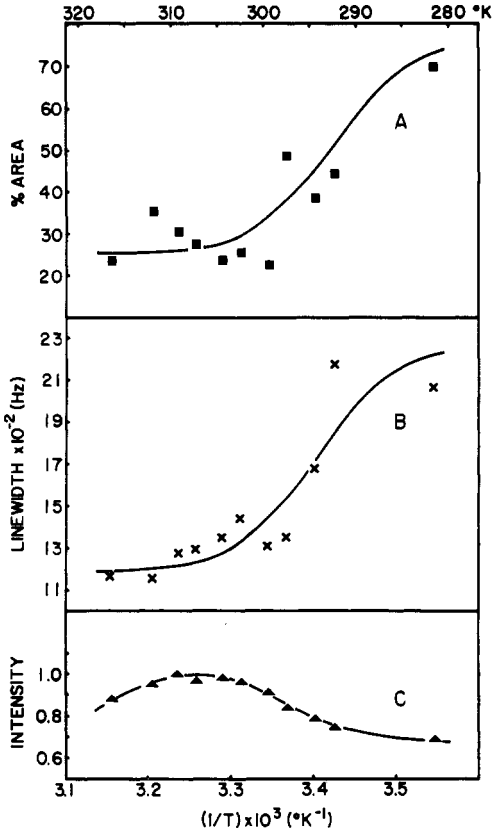

FIGURE 5: (A) Increase in percent area of the broad spectral component of the 8-FDPPC resonance as a function of the inverse temperature. The data were obtained by simulating the 8-FDPPC line shape with two Lorentzians. The computer then calculated the relative areas of the simulated peaks. The curve through the points is the same as that drawn through the points in (B). (B) ^{19}F-NMR line widths of the broad components of the 8-FDPPC spectra (see Figure 4) plotted as a function of inverse temperature. (C) Relative total intensities of the 8-FDPPC peak as a function of temperature. The 8-FDPPC resonances were integrated and then normalized to the maximum intensity at 310 K. The curves through the data points in Figures 5 and 6 were drawn to indicate a leveling off at low temperature to be consistent with the data for 8-FDPPC (Figure 6C), which had the highest signal to noise ratio.

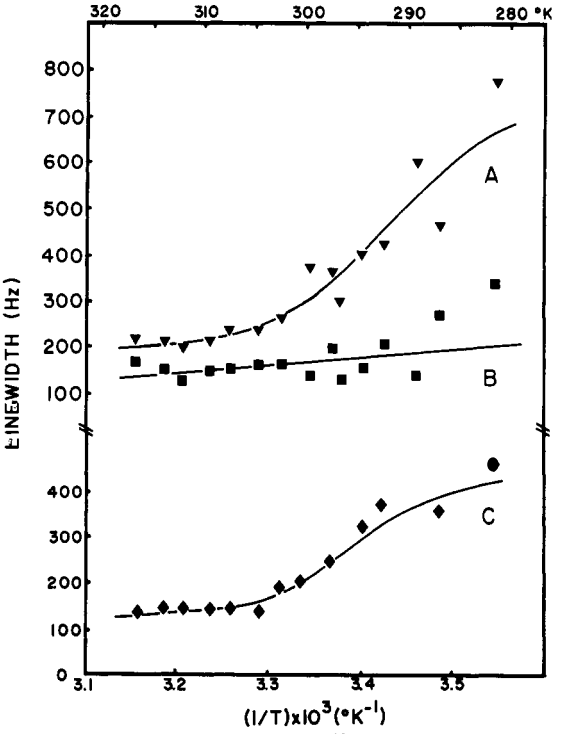

FIGURE 6: Narrow components of the ^{19}F resonance line widths of F-Phe- and F-Tyr-labeled M13 coat protein reconstituted into 8-FDPPC-labeled vesicles (see Figure 4) plotted as a function of the inverse temperature: (A) F-Tyr; (B) F-Phe; (C) 8-FDPPC. The curves through the data points in Figures 5 and 6 were drawn to indicate leveling off at low temperature to be consistent with the data for 8-FDPPC (C), which had the highest signal to noise ratio.

the resonances at 317 K may be approximately fit with a single Lorentzian curve. At 292 K, however, this is not possible; there is a "broad" component underneath the "narrow" component. To improve the signal to noise of the 8-FDPPC resonance to allow a quantitative analysis of the spectra, vesicles were prepared with a high concentration of the 8-FDPPC. The resulting 8-FDPPC spectra at 317 and 292 K are shown in the insets of Figure 4. All of the 8-FDPPC spectra in the temperature series were analyzed as the sum of two Lorentzians and the relative contribution of the broader component to the total area of the 8-FDPPC resonance as a function of temperature is shown in Figure 5A. As well, the line width of the broad component of the 8-FDPPC resonance as a function of inverse temperature is shown in Figure 5B. There is a certain amount of error in the measurements, but the trend is readily apparent: as the temperature is lowered through the phase transition of the DMPC (24 °C), there is a trend toward the broad component. This trend is reversible as the temperature was varied pseudorandomly. The behavior of the line width of the broad component of the 8-FDPPC resonance with temperature also reflects the phase-transition temperature of the DMPC, as does the line width of the narrow component (see below).

To determine whether we were seeing all of the 8-FDPPC signal, the area of the 8-FDPPC resonance was measured as a function of temperature. The results are shown in Figure 5C. The spectral parameters were the same for all the spectra collected. A significant decrease in intensity is observed below, and a slight decrease above, 310 K. The decrease in intensity below 310 K is interesting as the inflection point of the curve is near the T_m of the DMPC, 297 K. Again, this behavior is reversible as the points were obtained pseudorandomly.

To study the correlation between temperature and the line width of the narrow components for F-Phe, F-Tyr, and 8-FDPPC, the line widths of the narrow components were plotted as a function of the inverse temperature in Figure 6. The melting temperature (T_m) of the DMPC is 3.367×10^{-3} K^{-1} on these graphs. Curves 6A and 6B show the effect of temperature on F-Tyr and F-Phe resonances, respectively, of labeled protein in vesicles while curve 6C shows the simultaneous effect of temperature on the 8-FDPPC. As the temperature is lowered from 317 K (3.155×10^{-3} K^{-1}), the line widths of all three resonances initially broaden linearly with reciprocal temperature. As the T_m of the DMPC is approached, the increase in the line widths of the F-Tyr and 8-FDPPC resonances becomes nonlinear, and the line widths increase dramatically. The increase in line width of the F-Phe resonance remains linear throughout the temperature range measured, within experimental error.

The NMR spectral data required for motion analysis include $\Delta\nu$ and NOE measurements. These data for F-Phe- and F-Tyr-labeled coat proteins reconstituted into vesicles are given in Figure 7 and Table I. These measurements were taken at 303 K where the resonances are dominated by the narrower component (see above). The line widths were measured at 141, 254, and 376 MHz, while the T_1's and NOE's were collected at 141 and 254 MHz. The T_1's were obtained by the progressive saturation method in the absence of any ^{1}H irradiation (Hull & Sykes, 1975b). The NOE's result from irradiation

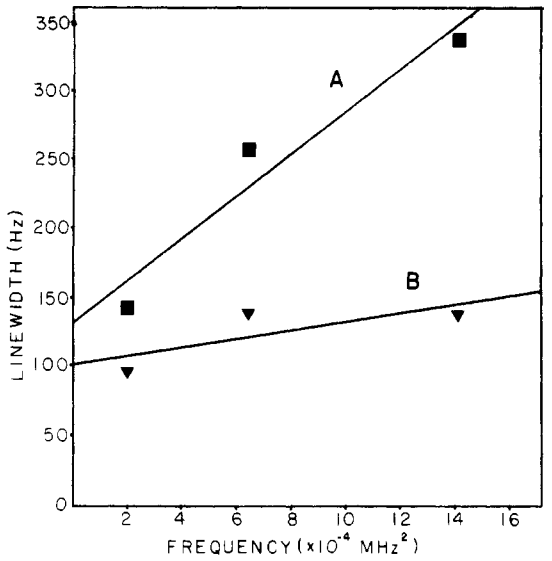

FIGURE 7: ^{19}F NMR line widths for (A) F-Tyr- and (B) F-Phe-labeled coat proteins in vesicles plotted as a function of the square of the spectrometer frequency at 303 K. The spectral parameters for the measurements were as follows: The 141-MHz (1.99×10^4 MHz^2) spectrum was the result of 15 000 scans with a 25-μs (78°) pulse, a ±10 000-Hz sweep width, 8K data, and a 300-ms delay between transients; the 254-MHz (6.45×10^4 MHz^2) spectral data were as listed in Figure 4; the 376-MHz (14.17×10^4 MHz^2) spectrum was obtained from 60 000 scans with a pulse width of 10 μs (75°), a sweep width of ±20 000 Hz, 8K data, and a delay of 300 ms between transients.

Table I: T_1 and NOE Data of F-Phe- and F-Tyr-Labeled Coat Proteins Incorporated into Vesicles

	T_1 (s)[a]	
frequency (MHz)	F-Phe	F-Tyr
141.178	0.43	0.52
254.025	0.50	0.52
	NOE[a]	
frequency (MHz)	F-Phe	F-Tyr
141.178	−0.51	−0.40
254.025	−0.28	−0.46

[a] Measured at 303 K.

of the entire proton spectrum.

To determine the sizes of the vesicles in the NMR samples studied, an electron micrograph was taken. Figure 8 shows the size distribution obtained. The mean vesicle radius of 178 vesicles measured was 159 ± 63 Å.

Discussion

Chymotryptic Digestion. The chymotrypsin digestion studies give information as to the exposure and orientation of the M13 coat protein when reconstituted into phospholipid vesicles. Previously, studies have shown that chymotrypic digestion of the protein in DOC micelles resulted in cleavage at the three phenylalanines but not at either of the two tyrosines (Dettman et al., 1982). The authors concluded that the F-Tyr residues were within the hydrophobic core of the micelle and consequently were protected from the protease, while the F-Phe residues were outside the micelle and therefore exposed.

The situation for the vesicle-bound protein has been found to be similar in that the protein F-Phe residues are susceptible to chymotryptic cleavage while the F-Tyr residues are not. In this case, however, only half of the termini are exposed; the other half are in the internal space of the vesicle. This raises the question of protein orientation: is the protein oriented with

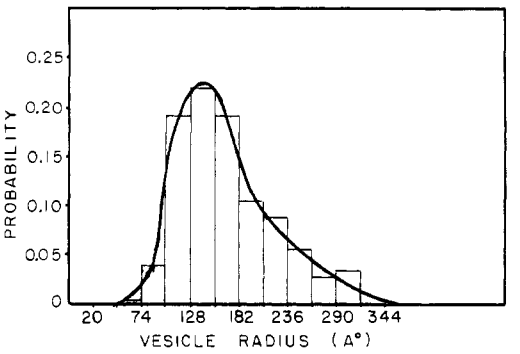

FIGURE 8: Histogram of vesicle size distribution of the labeled coat protein containing vesicles prepared. A total of 178 vesicles was measured from an electron micrograph. From the distribution obtained, it was calculated that any vesicle in the preparation has a 95% probability of having a radius between 20 and 327 Å. The mean radius is 159 ± 63 Å.

the N-termini on only one side of the membrane (asymmetrical orientation) or are the N- and C-termini distributed randomly on both sides of the bilayer (symmetrical orientation)? Paper electrophoresis of the hydrophilic fragments released shows that there is digestion of both the N- and C-termini. This indicates that the protein is symmetrically incorporated into the vesicle. Wickner (1976) has suggested that symmetrical orientation may also result from the protein being incorporated not transmembranously but in a "U" conformation. Experiments to determine the protein conformation(s) present in the vesicles prepared are being done.

Temperature Studies. In the temperature studies presented in this paper, two effects were seen as a function of temperature. First, the 8-FDPPC resonance in particular demonstrated the two- (multi-) component nature of the system with a broader resonance(s) dominating at lower temperature and a narrow resonance dominating at higher temperatures. Second, both narrow and broad components exhibited an intrinsic temperature sensitivity. Two possible explanations for the two- (multi-) state nature of the system are discussed herein: vesicle aggregation (without fusion) or phase separation due to the mixed lipid composition.

Evidence for the existence of reversible vesicle aggregation is found in two observations. First, it was qualitatively observed that as the temperature was lowered, the NMR sample became turbid, indicative of "larger particle" formation. Second, the comparison of the line widths of the broad components with those of the narrow components showed they were approximately 8 times larger at all temperatures. In the limit where the internal motions of the protein amino acid side chains are faster than the overall rotational correlation time for vesicle rotation, which certainly pertains to this situation, the line width of the resonance is directly proportional to the correlation time (Marshall et al., 1972) and, hence, to r^3 (see the Stokes–Einstein equation, below). This predicts that, if the broad component results from an aggregate of the monomeric vesicles, the ratio of the radii of the aggregates to that of the monomers should be given by

$$(\Delta\nu_{broad}/\Delta\nu_{narrow})^{1/3} = r_{broad}/r_{narrow}$$

For the data at all temperatures, the radius of the vesicles giving the broad component of the spectrum is calculated to be 1.94 ± 0.17 times that of the vesicles giving the narrow component.

In terms of this model, the decrease in intensity of the 8-FDPPC resonance below 310 K, shown in Figure 5C, is taken as evidence for higher orders of aggregation. If tetramers were formed, for example, their line widths would be

64 times that of the narrow monomer component, and they would be too broad to be observed. The decrease in intensity seen above 310 K where only the narrow component exists is most likely due to the expected change in T_1 with increasing temperature. As the temperature increases, the T_1 increases. The spectral acquisition parameters were constant throughout the entire temperature study so that as the T_1 increases, the resonances become more saturated.

Although the above discussion offers an explanation for the line-width data, Figure 5A shows that in the temperature range 282–317 K, there is never less than ~20% of the broad component present at the highest temperature. If the two-component phenomenon was purely a DMPC phase transition modulated aggregation, one would expect the curve to show all monomer above the T_m. That there is ~25% of the broad component present at 317 K raises the suspicion that the non-DMPC lipids (20% of the total lipid), whose T_m's are higher than 317 K, may actually be in pseudo-gel-state patches. This would result in two-component spectra. The presence of the narrow component at 282 K may be explained by typical behavior of small unilamellar vesicles [see Evans and Parsegian (1983)]. SUV's are strained spheres with high radii of curvature above the T_m of their lipids. As the temperature is lowered through the phase transition, the strain causes the spheres to become polygonal, to relieve the tension. The lipids in the interspace between the polygonal faces would have greater methylene chain mobility than those in the gel-state faces, and consequently, ^{19}F-labeled lipid (or protein) in these regions would result in the narrow components seen.

From the above discussion, it is unclear which model best explains the data. Regardless, it does not affect the validity of the motion analysis presented below as the data used were obtained from the narrow component at 303 K (above the DMPC phase-transition temperature) and therefore pertain to the protein in liquid-crystalline lipids in monomeric vesicles.

Analysis of Narrow Spectral Component Line Shapes. Upon inspection of Figure 8 showing the size distribution of the vesicles, it is obvious that the vesicles are a mixed population of sizes. As every size of vesicle will have its own characteristic correlation time and the line-width, T_1, and NOE results depend on the overall correlation time (see Theory), the measurements of these data are actually weighted averages according to the sizes of the vesicles and their relative probabilities in the vesicle population.

To determine the "weighted" effective overall correlation time corresponding to the observed data, the effect of the sample size heterogeneity on the line width was analyzed in the following manner. Correlation times at 303 K were calculated for each of the sizes of vesicles shown in Figure 8 by using the Stokes–Einstein equation $\tau_c = 4\pi r^3\eta/(3kT)$. These were used to calculate a Lorentzian line shape for each size [with the assumption that the line width is proportional to the overall correlation time (Marshall et al., 1972)]. These line widths were used in conjunction with their relative probabilities to simulate a "weighted" line shape. The simulated line shape was then measured in the same manner as the experimental data were analyzed, and a best fit line width was determined. This line width was used to calculate an effective "weighted" overall rotational correlation time of 1.9×10^{-6} s. This effective correlation time derived from T_2 measurements has also been used for the analysis of the T_1 and NOE data since the T_1 calculations are not sensitive to the exact choice of the overall correlation time (see Table II).

With the evaluation of the effective overall rotational correlation time, we are now in a position to analyze the measured relaxation parameters determined for the F-Tyr and F-Phe residues of the vesicle-bound protein. Quantitation of the motions of the F-Phe and F-Tyr residues was done by using a computer program based on the equations outlined under Theory. The rate of the diffusion about the $\alpha\beta$- and $\beta\gamma$-bonds (D_1 and D_2, respectively) and the wobble angle about the $\alpha\beta$-bond (γ_0) were varied to obtain the line width, T_1, and NOE values closest to the experimental data. The calculated values closest to the line width data at 254 MHz were chosen as these line widths were measured in six individual experiments and so are known with greater accuracy than the data at the other two frequencies, which were measured only once.

Table II: T_1, Line-Width, and NOE Data from the Best Fit Values of D_1, D_2, and γ_0[a]

	frequency (MHz)		
parameter	141	254	376
F-Tyr:	$D_1 = 2 \times 10^8$, $D_2 = 4 \times 10^8$, $\gamma_0 = 75°$, $\tau_c = 1.9 \times 10^{-6}$		
T_1	0.96 (0.52)	0.72 (0.52)	0.59
$\Delta\nu$	115 (143)	242 (257)	461 (336)
NOE	−0.18 (−0.40)	−0.17 (−0.46)	−0.13
F-Phe:	$D_1 = 2 \times 10^8$, $D_2 = 4 \times 10^8$, $\gamma_0 = 90°$, $\tau_c = 1.9 \times 10^{-6}$		
T_1	0.62 (0.43)	0.69 (0.50)	0.69
$\Delta\nu$	86 (96)	173 (139)	323 (138)
NOE	−0.15 (−0.51)	−0.26 (−0.28)	−0.27
F-Phe:	$D_1 = 2 \times 10^8$, $D_2 = 4 \times 10^8$, $\gamma_0 = 90°$, $\tau_c = 1.5 \times 10^{-6}$		
T_1	0.62	0.69	0.69
$\Delta\nu$	68 (96)	137 (139)	256 (138)
NOE	−0.15	−0.26	−0.27

[a] The experimentally determined data are given in parentheses.

It was found that the calculated T_1, line width, and NOE's for F-Tyr were closest to those obtained experimentally when $D_1 = 2 \times 10^8$ s^{-1}, $D_2 = 4 \times 10^8$ s^{-1}, and $\gamma_0 = 75°$. The line-width data agree quite well, but the calculated T_1's are too long (see Table II). This indicates that some rapid intermolecular interactions must also be present. Such an interaction could be between the F-Tyr and passing lipid chains (Hagen et al., 1978). This would decrease the T_1 value but would have negligible effect on the line width.

The best fit values for the F-Phe data were $D_1 = 2 \times 10^8$ s^{-1}, $D_2 = 4 \times 10^8$ s^{-1}, and $\gamma_0 = 90°$ (Table II). In this case, however, neither the line widths nor T_1's fit the data very well. That the calculated line widths are too large indicates additional motion is present that is not included in the model. This implies that the hydrophilic ends must have more backbone motion allowed than the hydrophobic domain. The effect of this would be to decrease the overall correlation time of the vesicle (as far as the F-Phe are concerned). The results of a simulation with the overall correlation time reduced from 1.9 $\times 10^{-6}$ to 1.5 $\times 10^{-6}$ s is shown in Table II. The line widths now are closely simulated. The T_1's are still too long, however. Intermolecular interactions are again indicated. In this case, the fluorine could be experiencing dipolar interactions with either the phospholipid head groups of the lipid or other protein residues. The NOE's in both the F-Phe and F-Tyr cases do not fit very well. This is expected as the NOE calculations depend upon the T_1 values. Since the T_1 values do not fit well, then the NOE's will not either.

Motional Analysis of F-Phe- and F-Tyr-Labeled Coat Protein in Vesicles: Influence of Lipids. The F-Tyr and 8-FDPPC line widths are markedly dependent on the fluidity state of the DMPC (Figure 6). It seems that the rigidity of the hydrocarbon chains of the DMPC gel state decreases the internal motions of the F-Tyr ring and 8-FDPPC chain. As well, the decrease of the translational diffusion of the lipids

upon forming a gel state would allow an increase in dipolar interaction between the F-Tyr or 8-FDPPC fluorine nuclei and neighboring lipid protons. This would also contribute to the broadening of the respective fluorine resonances.

Conclusions

These studies have outlined an overall picture for the M13 coat protein's interaction with lipids when reconstituted into phospholipid vesicles. The rotations of the tyrosine residues in the hydrophobic domain of the protein, although not greatly restricted by the lipids, are still influenced by them. Above the T_m of the lipids, the motional properties of the side chains of the F-Tyr residues in the portion of the protein surrounded by lipids are very similar to those found for typical globular proteins in aqueous solution (Hull & Sykes, 1975a). The F-Phe residues, as markers of the hydrophilic regions of the protein, were found to be only slightly more mobile than the tyrosines. This finding indicates that the hydrophilic ends are not "waving" around in solution but must be either structured or associated with the phospholipid head groups.

Acknowledgments

We thank Drs. Ponsy Lu and Stan Opella for the use of their 150-MHz spectrometer, Dr. T. Nakashima and Glen Bigam for the 376-MHz spectra, Dr. Ruthven Lewis for synthesizing the 8-FDPPC, Roger Bradley for taking the electron micrographs, Dr. Larry Smillie for the continued use of his amino acid analysis facilities, and M. Nattriss for the amino acid analyses.

Registry No. Phe, 63-91-2; Tyr, 60-18-4; DMPC, 13699-48-4; DPPA, 19698-29-4; 8-FDPPC, 86569-18-8.

References

Cross, T. A., & Opella, S. J. (1979) *J. Supramol. Struct. 11*, 139.

Cross, T. A., & Opella, S. J. (1980) *Biochem. Biophys. Res. Commun. 92*, 478.

Cross, T. A., & Opella, S. J. (1981) *Biochemistry 20*, 290.

Dettman, H. D., Weiner, J. H., & Sykes, B. D. (1982) *Biophys. J. 37*, 243.

Evans, E. A., & Parsegian, V. A. (1983) *Ann. N.Y. Acad. Sci.* (in press).

Gall, C. M., DiVerdi, J. A., & Opella, S. J. (1981) *J. Am. Chem. Soc. 103*, 5039.

Gall, C. M., Cross, T. A., DiVerdi, J. A., & Opella, S. J. (1982) *Proc. Natl. Acad. Sci. U.S.A. 79*, 101.

Hagen, D. S., Weiner, J. H., & Sykes, B. D. (1978) *Biochemistry 17*, 3860.

Hagen, D. S., Weiner, J. H., & Sykes, B. D. (1979a) *Biochemistry 18*, 2007.

Hagen, D. S., Weiner, J. H., & Sykes, B. D. (1979b) in *NMR and Biochemistry* (Opella, S. J., & Lu, P., Eds.) p 51, Marcel Dekker, New York.

Hartree, E. F. (1972) *Anal. Biochem. 48*, 422.

Hull, W. E., & Sykes, B. D. (1974) *Biochemistry 13*, 3431.

Hull, W. E., & Sykes, B. D. (1975a) *J. Mol. Biol. 98*, 121.

Hull, W. E., & Sykes, B. D. (1975b) *J. Chem. Phys. 63*, 867.

Jardetzky, O., & Roberts, G. C. K. (1981) in *NMR in Molecular Biology*, Chapter 12, Academic Press, New York.

Kinsey, R. A., Kintanar, A., & Oldfield, E. (1981) *J. Biol. Chem. 256*, 9028.

London, R. E. (1980) in *Magnetic Resonance in Biology* (Cohen, J. S., Ed.) Chapter 1, Wiley Interscience, New York.

Makino, S., Woolford, J. L., Jr., Tanford, C., & Webster, R. E. (1975) *J. Biol. Chem. 250*, 4327.

Marshall, A. G., Schmidt, P. G., & Sykes, B. D. (1972) *Biochemistry 11*, 3875.

Raheja, R. K., Kaur, C., Singh, A., & Bhatia, I. S. (1973) *J. Lipid Res. 14*, 695.

Weiner, J. H., & Sykes, B. D. (1980) in *Magnetic Resonance in Biology* (Cohen, J. S., Ed.) Vol. 1, p 171, Wiley Interscience, New York.

Wickner, W. (1976) *Proc. Natl. Acad. Sci. U.S.A. 73*, 1159.

Wittebort, R. J., & Szabo, A. (1978) *J. Chem. Phys. 69*, 1722.